U.S. DEPARTMENT OF COMMERCE
Peter G. Peterson, Secretary

NATIONAL OCEANIC AND ATMOSPHERIC ADMINISTRATION
Robert M. White, Administrator

ENVIRONMENTAL RESEARCH LABORATORIES
Wilmot N. Hess, Director

NOAA TECHNICAL REPORT ERL 234-POL 11

Juan de Fuca Ridge and Sovanco Fracture Zone RP-5-OC-71

WILLIAM H. LUCAS

BOULDER, COLO.
May 1972

For sale by the Superintendent of Documents, U. S. Government Printing Office, Washington, D. C. 20402
Price 50 cents

Table of Contents

JUAN DE FUCA RIDGE AND SOVANCO FRACTURE ZONE

RP-5-OC-71

William H. Lucas

Profiles and contour maps of bathymetry, gravity and magnetics along 20 lines, 105 KM long, comprising a 10 x 10 point grid over the intersection of the northern end of the Juan de Fuca Ridge and Savanco Fracture Zone are presented and discussed. A summarized description of shipboard operations of approximately 2400 KM of continuous seismic profiling, 100 heat flow stations, 8 cores and 4 camera stations are also given.

1. INTRODUCTION

1.1 Purpose

The purpose of RP-5-OC-71 cruise was (1) to locate a 10 x 10 point grid of heat flow stations at the intersection of the northern end of the Juan de Fuca Ridge and the Sovanco Fracture Zone, and to obtain heat flow measurements from this grid, (2) to map the bathymetry, basement topography, magnetic, and gravity characteristics of the area covered by the grid, and (3) to relate the obtained information to the local structure of the Pacific Plate-Juan de Fuca Plate boundary.

The cruise was conducted jointly by the NOAA Pacific Oceanographic Laboratories and the Department of Oceanography of the University of Washington. The project was conducted aboard the NOAA Ship OCEANOGRAPHER from 24 August to 10 September and 13 September to 1 October, 1971.

Dr. Robert E. Burns, Pacific Oceanographic Laboratories, was Project Supervisor and served as Chief Scientist during the first half of the operation. William H. Lucas, Pacific Oceanographic Laboratories, was Chief Scientist during the second half of the operation. In addition, Dr. Clive Lister, Mr. Earl Davis, Mr. Mark Miller and Mr. Doug Johnson of the University of Washington participated as part of the joint research project.

1.2 Geologic Setting

Present hypotheses of plate tectonics suggest that most tectonic activity is confined to relatively narrow zones which form boundaries between rigid lithospheric plates. Although the rising and spreading associated with thermal convective cells in the upper mantle has been proposed as a possible driving force for divergent plate movements, actual measurement of heat flow through the sea floor has been very difficult in areas of active spreading centers. In these

areas, a wide variability is generally observed in measured heat flow values, particularly in the rugged areas of the mountainous types of mid-ocean rise.

In contrast with the generally rugged topography and the relatively sparse and irregular sediment cover at most active spreading centers, the northern end of the Juan de Fuca Ridge westward along the Sovanco Fracture Zone to the Explorer Trough is covered by a relatively thick blanket of turbidites. This provides an ideal situation in which to systematically sample the heat flow of the region, without the problem of having to locate measurements specifically on the basis of where there is adequate sediment to permit penetration. In addition, the sampling design was established to permit statistically valid interpolation of the results by eliminating the normally introduced bias imposed by having to search for a location where a measurement is possible.

1.3 Location

The project was conducted within the area bounded by 48° and 50°N, 128° and 130°W (fig. 1). It required the development of a 100 x 100 kilometer grid (10 x 10 station points at 10 kilometer spacing). Although an approximate

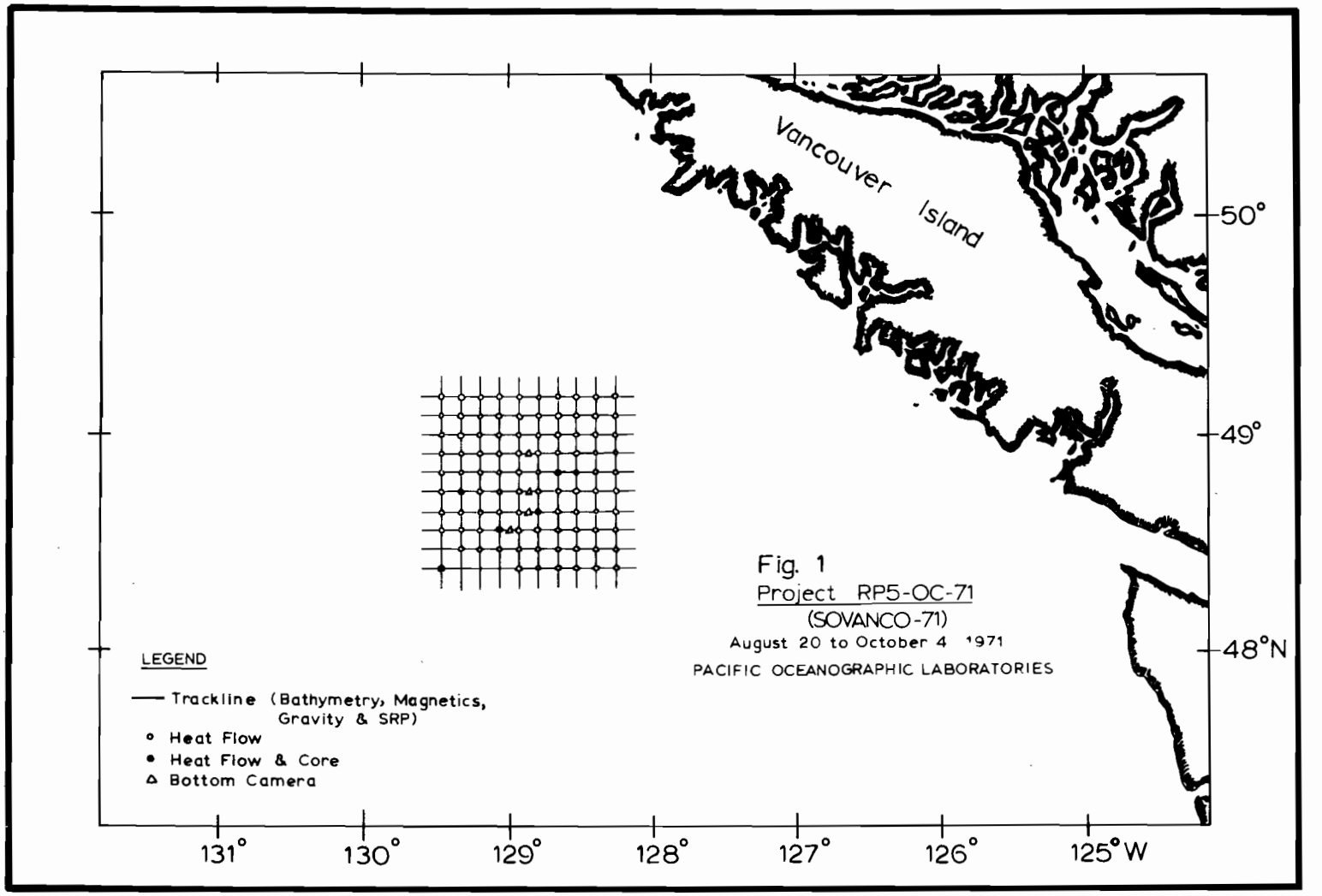

Figure 1. Map showing location of the 100 x 100 kilometer grid over the northern end of the Juan de Fuca Ridge and intersection of the Sovanco Fracture Zone.

specific location of the stations comprising the grid were based on additional information developed during the initial phase of the project.

2. DATA REDUCTION

2.1 Field Methods and Data Processing

Time, bathymetry, magnetic, and gravity values were logged in real time by a Raw Data Logger on punched paper tape. This tape was later translated by the computer into a Raw Data tape in which the 5-minute manual depth entry delay was removed as well as the inherent 5-minute delay in gravity values. Printouts of the Raw Data tape were annotated with corrections, omissions, and insertion of peaks and deeps. From the annotated data a corrector tape was prepared. Gravity meter shaft encoder corrections and cross-coupling corrections were logged on a shaft tape while periods during which the gravimeter was secured are logged on a status tape.

The Raw Data, Corrector, Shaft, and Status tapes were then processed together to generate the Edited Data Tape. In this process a 3 fathom draft correction was added to the depth values.

A Position Tape was prepared from the coordinates of the fixes on the smooth plotted boat sheets and processed to produce a printout of course and speed between positions. Sufficient positions were used to delineate the track and to keep the interval between positions below a maximum of 1-1/2 hours. Smooth plot or logging errors were identified and the final Control Tape prepared. The Edited Data Tape and Control Tape were merged to obtain the Geophysical Report and the paper tape for profile plotting aboard the ship.

The primary data products of this procedure are 2 punched paper tapes and one printout.

(1) Edited data tape containing corrected records of time, depth, magnetics, and gravity, each at a basic five minute sample rate but with bathymetric peaks and deeps inserted as necessary.

(2) Control tape containing the time and position for all fixes used in the Position tape as well as the computed values of the International Geomagnetic Reference Field (IGRF) and the course and speed between the positions.

(3) Geophysical report listing the final processed data.

2.2 P.O.L. Data Processing

The bathymetric, gravity and magnetic data were further processed and edited at the Pacific Oceanographic Laboratory (POL), located at Seattle, Washington.

Following several edit procedures, the geophysical and navigation data furnished by the ship were transferred to punch cards using a 1620 computer. From these cards, as a further edit procedure, the computed ship's velocity between successive position fixes has been computed using a CDC 6400 computer which was also programmed to transfer the data from cards to magnetic tapes, to calculate positions by time interpolation between navigation fixes, to convert fathoms to meters, and to compute free-air anomalies.

3. TRACKLINE OPERATIONS

A total of 20 tracklines were completed, each 105 km in length. The East-West tracklines were numbered 1 through 10 with prefix E, starting from the North. The North-South tracklines were numbered 1 through 10 with prefix N, starting from the West (fig. 2).

Bathymetry, magnetic, gravity and SRP measurements were made along all lines. Two lines were run twice: line N8 because the SRP was inoperative during the first run,

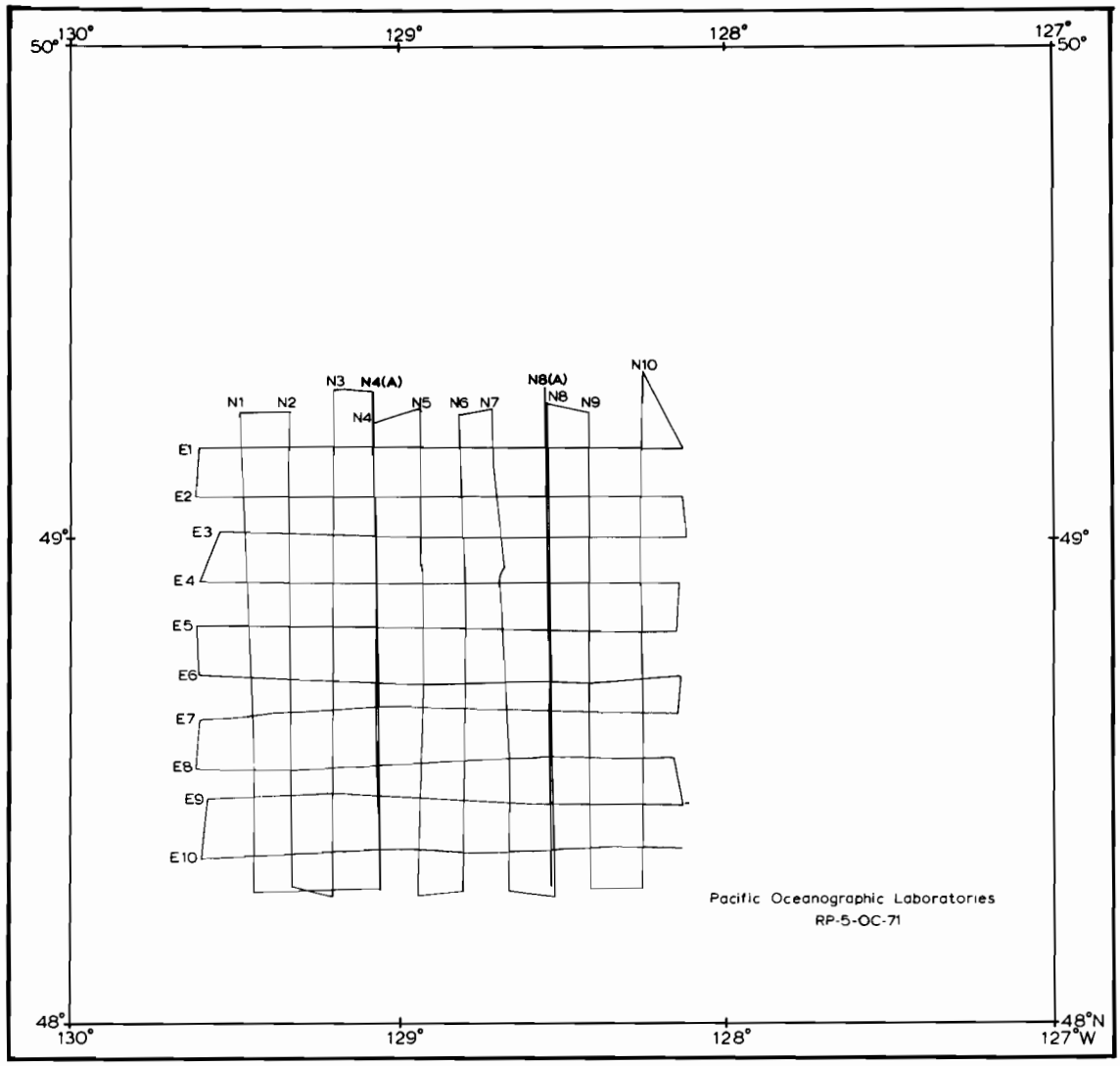

Figure 2. Map showing the ship's track along which bathymetry, gravity, magnetic, and seismic profiling information were collected.

line N4 because SRP data were not acceptable on the first run due to a noisy hydrophone array. A comparison of the underway geophysics for these 4 lines is shown in figures 3 and 4.

3.1 Depth Measurements

Bathymetric data (12 kilohertz) were obtained using an Edo (model 33A) recorder and either an Edo (model 248A) or Raytheon (PTR model 105) transceiver. Exceptionally good weather and sea conditions prevailed throughout most of the project and satisfactory soundings were made.

3.2 Magnetic Measurements

Magnetic data were collected using a Varian V4937 Direct Reading Proton Magnetometer. The sensing head was towed 650 feet behind the ship. The analog recorder was run at 6 inches per hour and the timing cycle polarization was 60 seconds except during testing and tuning.

Data were logged continuously on an analog trace and five minute intervals on punch paper tape. They were later reduced by subtracting the International Geomagnetic Reference Field (IGRF 1965) values for the corresponding location. Data quality was generally excellent.

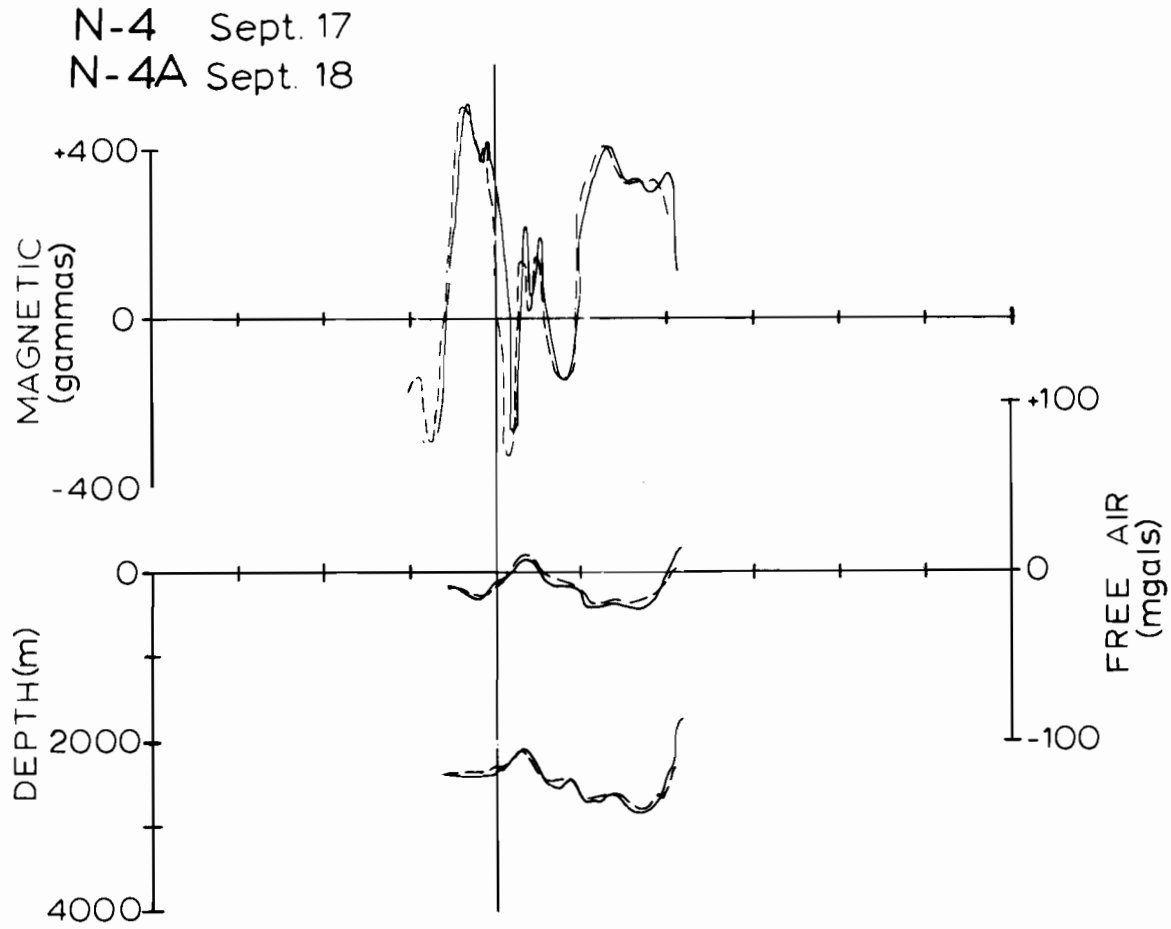

Figure 3. Comparison of the bathymetry, free-air gravity and magnetic profiles along lines N-4 and N-4A. Small dashes were used to outline N-4A (see fig. 2 for location of profiles).

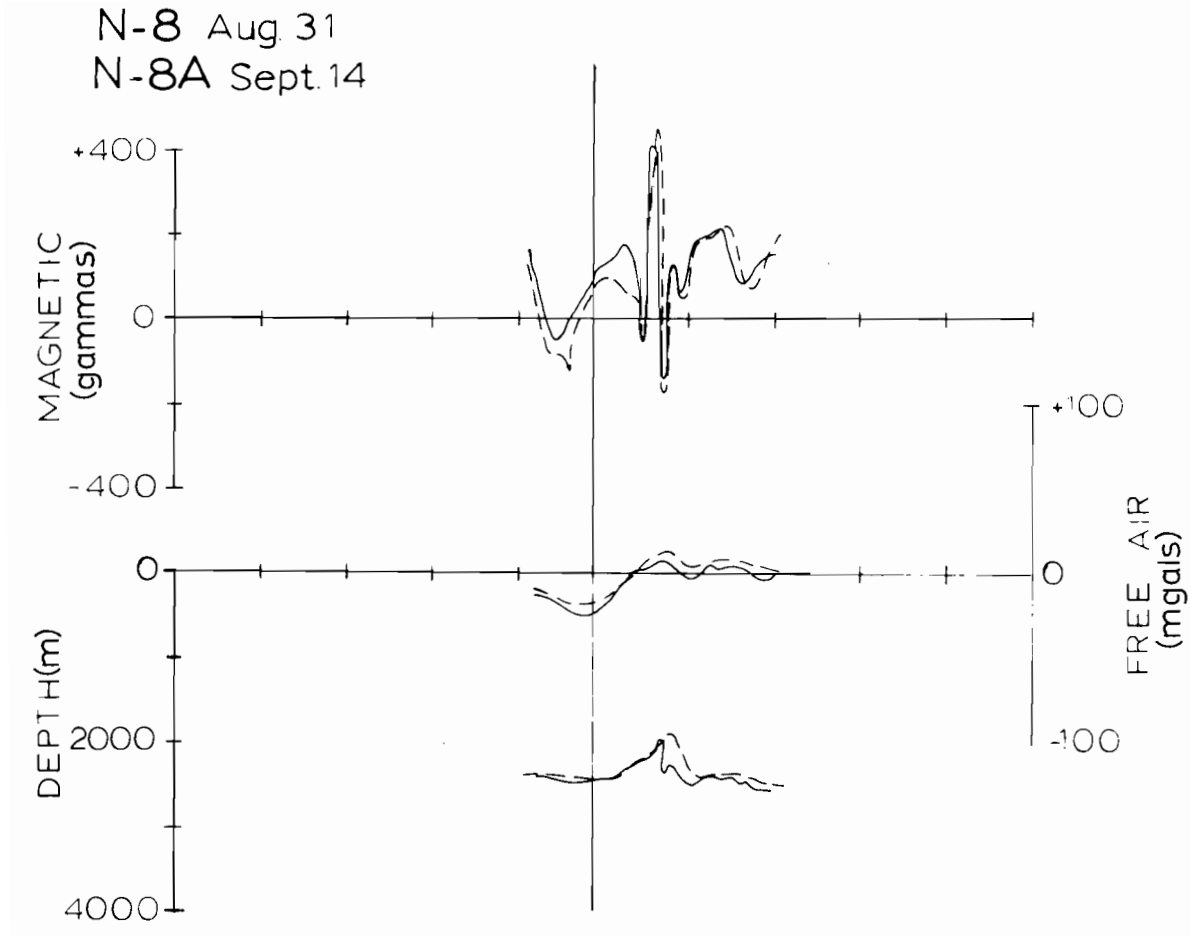

Figure 4. Comparison of the bathymetry, free-air gravity and magnetic profiles along lines N-8 and N-8A. Small dashes were used to outline N-8A (see fig. 2 for location of profiles).

3.3 Gravity Measurements

The Askania GSS2 gravity meter operated satisfactorily for the entire project. Sea conditions were good during the period the meter was operated. One hundred twenty trackline crossings were obtained on the grid pattern, and results show that crossing errors were quite low, averaging about 2.4 mgal. The Cape Flattery gravity range was crossed on October 1 using Satellite and Loran-A for navigational control. Gravity values obtained were 0 to 2 mgals low, averaging -1.4 mgal. This is well within the expected range of error due to navigation where an error of 0.3 kt. in computed speed introduces an error of 1.5 mgal.

The land tie at Port Angeles at the end of the first phase showed a drift of +0.6 mgal, and the land tie at PMC at the end of the project showed an additional +1.5 mgal drift. Corrections were applied to the data assuming the drift rate to be linear. The long term component of the cross-coupling correction was incorporated during the final reduction of the gravity data.

3.4 Seismic Reflection Profiling

Approximately 2400 KM of continuous seismic profiling was completed employing an electromagnetic bubble-pulse

transducer operating at 170 Hz with an output of 300 joules. Individual pulses consisted of 1-1/2 cycles at 170 Hz and were emmitted at a 5 second repitition rate. The incoming reflected signal was correlated with a fixed signal simulating the outgoing pulse. Penetration of up to 1-1/2 seconds in sediment was achieved.

The sound source transducers were lowered into the water from the upper (F) deck, using the crane, and towed by a cable from the lower (E) deck. The hydrophone steamers were towed from the port side boom on (E) deck. Underway operating speed was typically 7 knots (64 RPM). Excellent records were obtained on 20 tracklines.

4. STATION OPERATIONS

The Seismic Reflection Profiling and station data are being analysed at the University of Washington. The results of these data will be published in the scientific literature.

Station operations consisted primarily of heat flow measurements interspersed with coring and bottom camera observations. All occupied stations were numbered consecutively and the successful stations are shown in a schematic location diagram in figure 5. The exact location of all stations are given Appendices A, B and C.

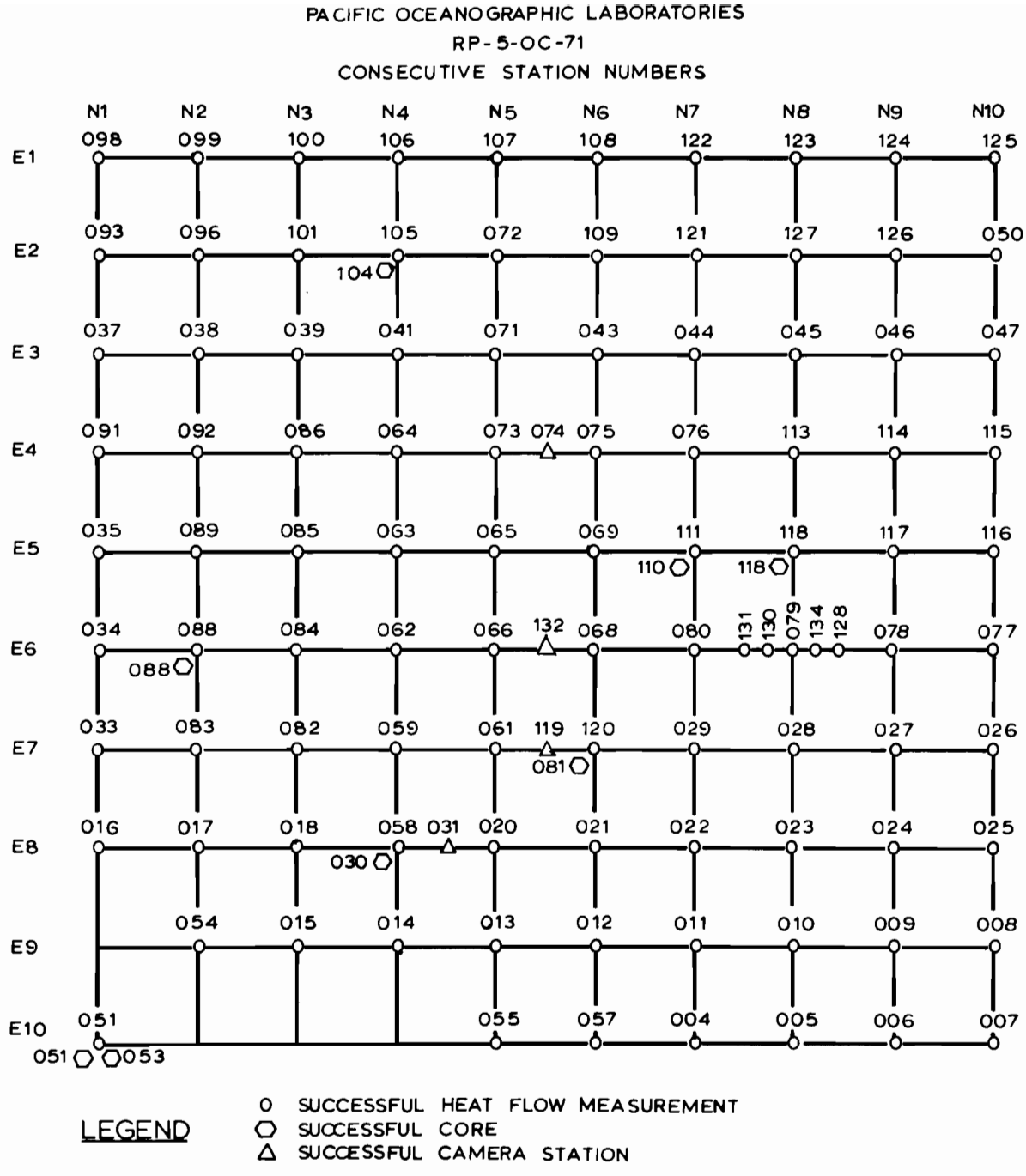

Figure 5. Diagram showing successful heat flow measurements, cores and camera stations (see Appendices A, B, and C for exact location of stations).

All equipment was lowered over the stern from the (E) deck A-frame. The oceanographic winches with 3/16 inch wire were used for the heat probe and camera, the deep sea winch with its tapered cable for the coring operations.

4.1 Heat Flow

Heat flow measurements were made using two techniques. The preponderance of stations were made using a modified (Bullard type) heat flow probe capable of measuring the sediment thermal conductivity in situ. The apparatus consists of a 1 cm. diameter probe 2 meters long, containing thermistors and a manganin heater wire, mounted beneath the digital punched tape recorder and power supply. The upper and lower thermistors, separated by 182 cm., provide the thermal gradient measurement; the gradient linearity is checked by the central 25 thermistor string. Average conductivity is determined by the heating curves of all sensors during the 20 minute period of constant heat supply. A total bottom time of 30 minutes is required for a complete measurement. The gradient is determined in 10 minutes, necessary for sufficient decay of frictional heating from impact, and the conductivity is determined in 20 minutes. Relative temperatures are recorded to .001° precision and are

displayed in analog format upon retrieval of the tape after station completion. The details of this apparatus and the methods used are given by Lister (1970).

The second technique of heat flow measurement utilizes the same recording apparatus but used three outrigger thermistor probes mounted at approximately 1.5 meter spacing on the gravity corer. An in-bottom time of 10 minutes is required as only the gradient is measured. Conductivity must be determined on the core sample by either needle probe or water content procedure. The location for these stations are given in Appendix A (sta. 45, 51, 88 and 118).

4.2 Coring

Most coring was accomplished with a 3 inch diameter gravity corer 15 feet long. The 1200 lb. weight was slotted to accept the digital heat flow recorder.

To obtain a large volume core for radio carbon dating purposes a 6 inch diameter 10 foot long gravity corer was used in one pelagic sedimented location (Appendix B, station 6C053). Some difficulty was experienced in obtaining core samples due to malfunction of the core catcher, but all 8 planned cores were obtained.

Four successful camera stations were made using a 16 mm Cine movie camera. A thallium iodide lamp synchronized with the shutter provided illumination. Optimum height for flying the camera with this illumination was 10 to 15 feet above the bottom. At the rate of 5 frames/sec., 100 feet of film provided 20 minutes of exposure. A drift velocity of about 1/2 knot was usually attempted. Locations are given in Appendix C.

4.4 Navigation

Navigation was accomplished with data obtained from the AN/SRN-9 Satellite Navigation system and supplemented by Loran A and C. This system was nearly trouble-free for the entire project and the resulting position control within the grid area is excellent. The short connecting lines where the ship was turning and maneuvering to occupy the next line are less accurate and subject to small errors in the absolute position.

5. INTERPRETATION

The purpose of this report is to present a summary of the information gathered during the project and the

preliminary results of the bathymetry, gravity and magnetics. To estimate the accuracy of the survey, differences in values for bathymetry, gravity and magnetics at the 100 trackline intersections were compiled and analyzed. The bathymetry had only four intersections in which serious discrepancies appeared, however the contour map (fig. 10) revealed that these discrepancies occured in areas of steep gradients (i.e., Heck Seamounts) and are not due to positional inaccuracies. The average difference in gravity was 2.4 mgals. Since the magnetic data were not corrected for diurnal variations the higher cross-over values (approx. 30 gammas) can be accounted for by the amplitude of the diurnal variations in the survey area, and also by the amplitudes and lengths (gradients) of the magnetic anomalies.

5.1 Profile Presentation

This report presents objectively the bathymetric, gravity and magnetic data of this survey in profile form so that any feature can be located with relative accuracy and the relationship between these three parameters along trackline segments can be seen clearly. The profiles are labeled so they can be directly keyed to figure 2 for trackline locations.

The profiles are presented in two groups. The first set (figures 6 and 7) shows the free air gravity anomaly with the corresponding topography and the second set (figures 8 and 9) the magnetic anomalies with topography. Due to the large amplitude of the magnetic anomalies the scale for the second set is smaller.

5.2 Bathymetry

The bathymetric map of the area (fig. 10) is contoured on a 100 m interval. The most prominent bathymetric feature is the northend of the Juan de Fuca Ridge which appears as a double ridge with a median trough lying between 128° 30' and 129°W. The trough has a flat bottom indicating sediment fill. The two crests extend north by north-northeast to about 48° 50'N where they are disrupted by the east-west trends of the Sovanco Fracture Zone.

The Juan de Fuca Ridge appears in this region to be an area approximately 30 km wide with 400-500 m hills rising from a level of close to 2500 m. The Ridge is delimited on the west by a 700-800 m scarp. At the base of the scarp is a trough 5-6 KM wide, which appears to be a continuation of the intermontane valley north of the Heck Seamount Chain (McManus, 1967).

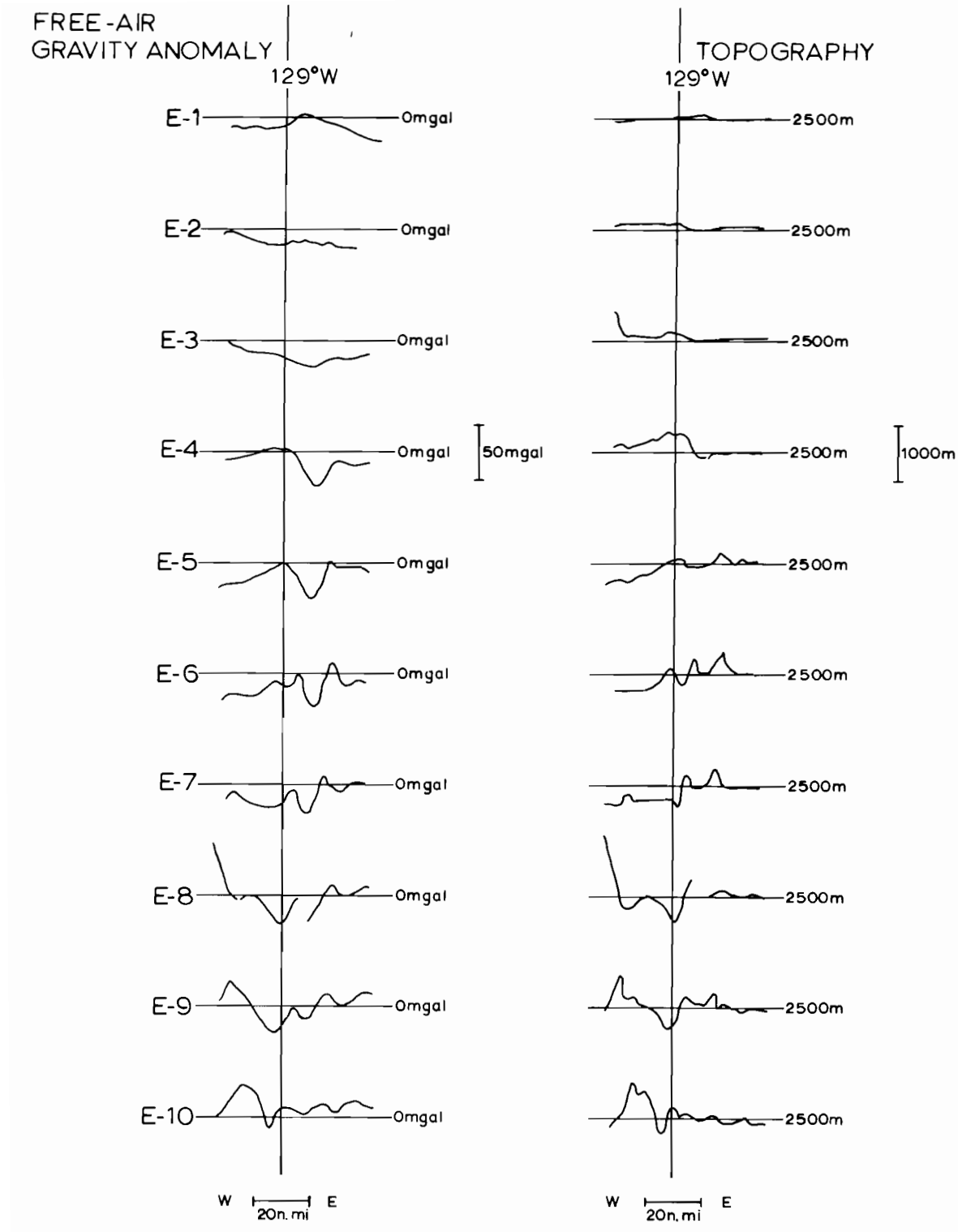

Figure 6. Alignment of the east-west free-air gravity and topography profiles (see fig. 2 for location of profiles).

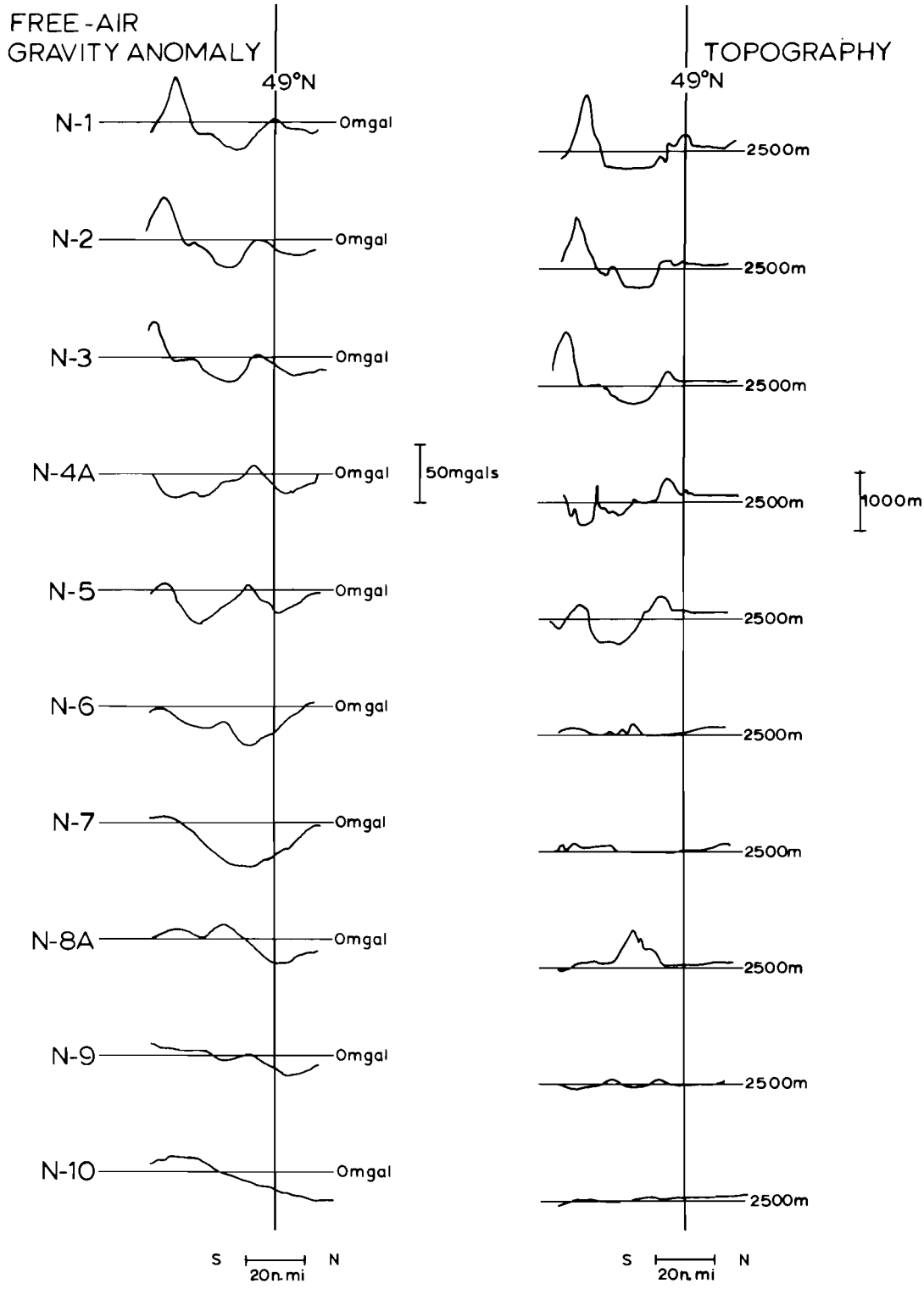

Figure 7. Alignment of the north-south free-air gravity and topography profiles (see fig. 2 for location of profiles).

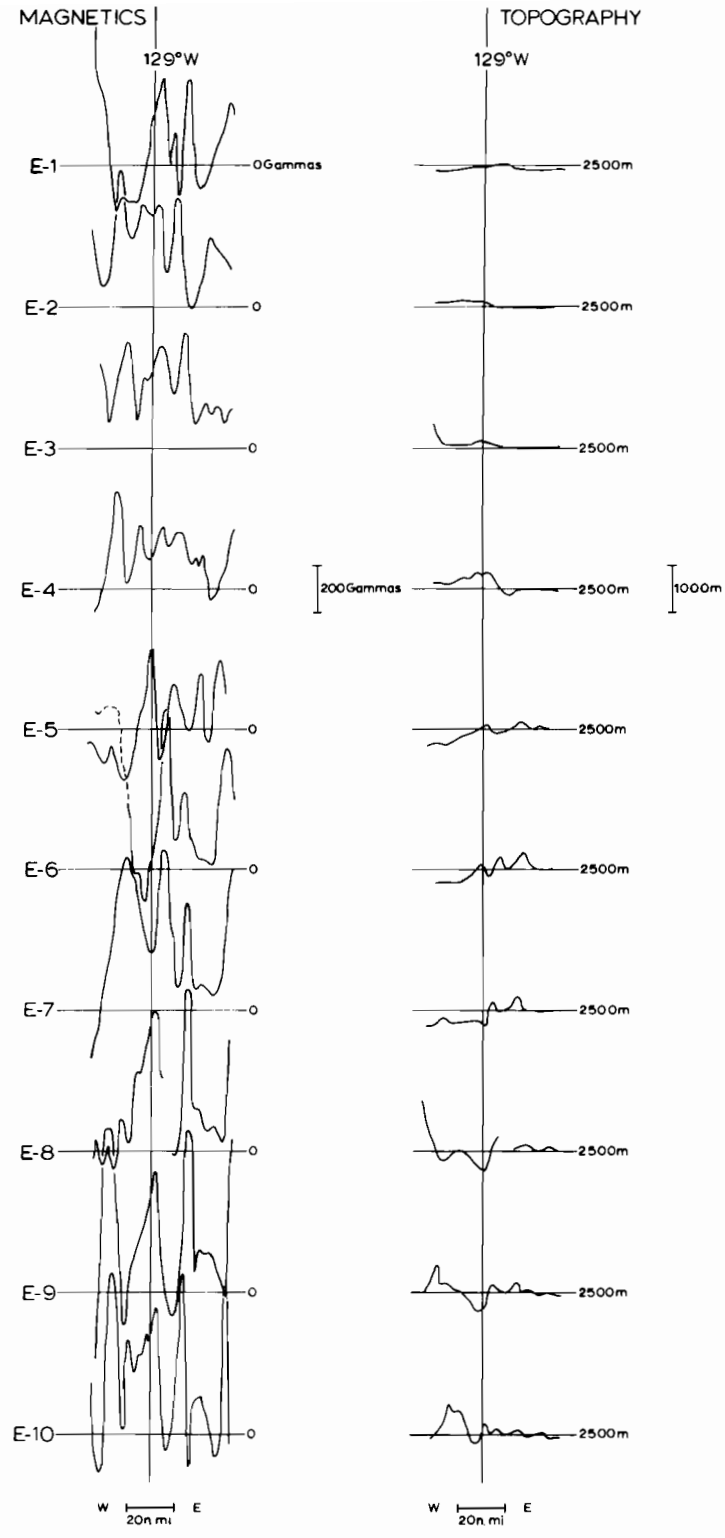

Figure 8. Alignment of the east-west magnetic and topography profiles (see fig. 2 for location of profiles).

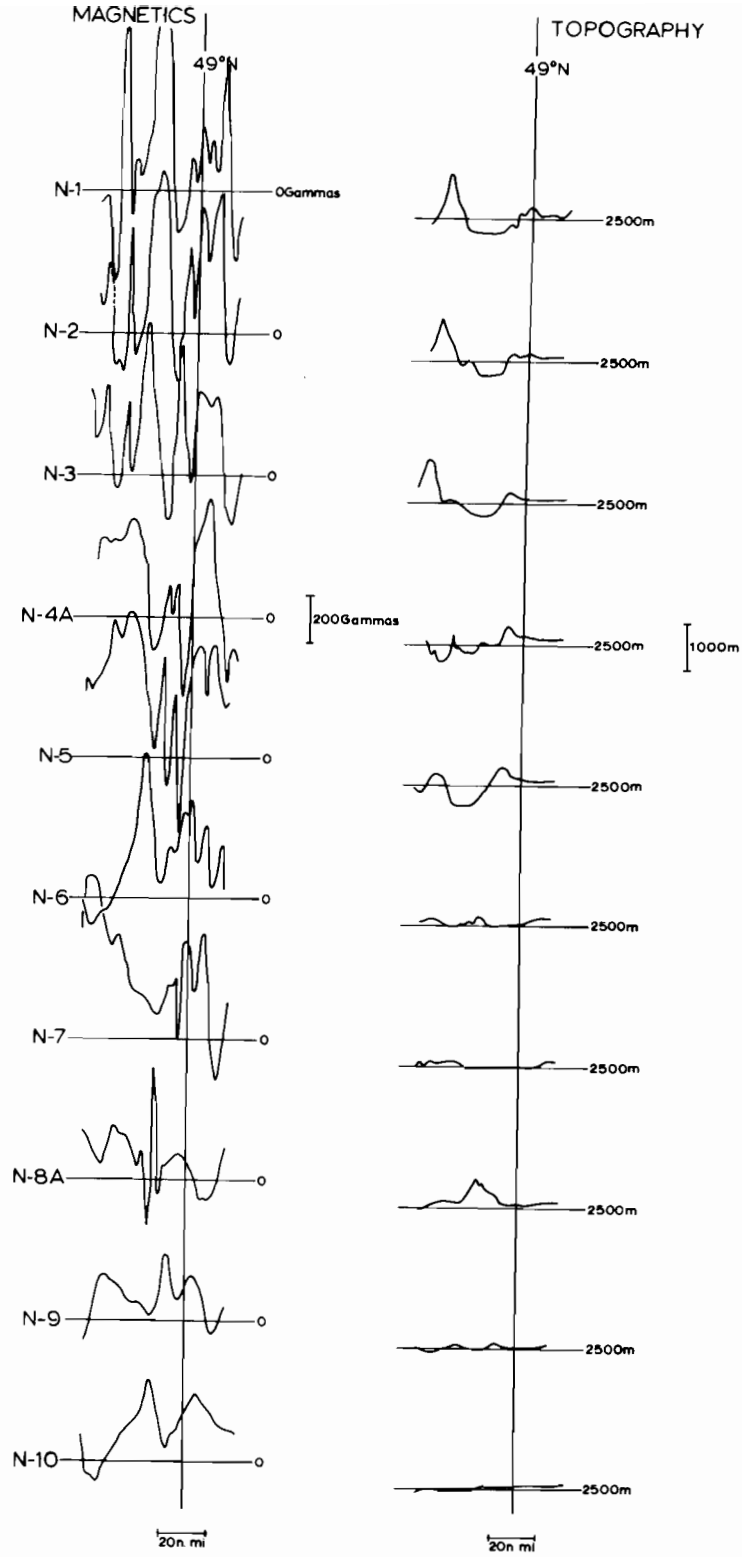

Figure 9. Alignment of the north-south magnetic and topography profiles (see fig. 2 for location of profiles).

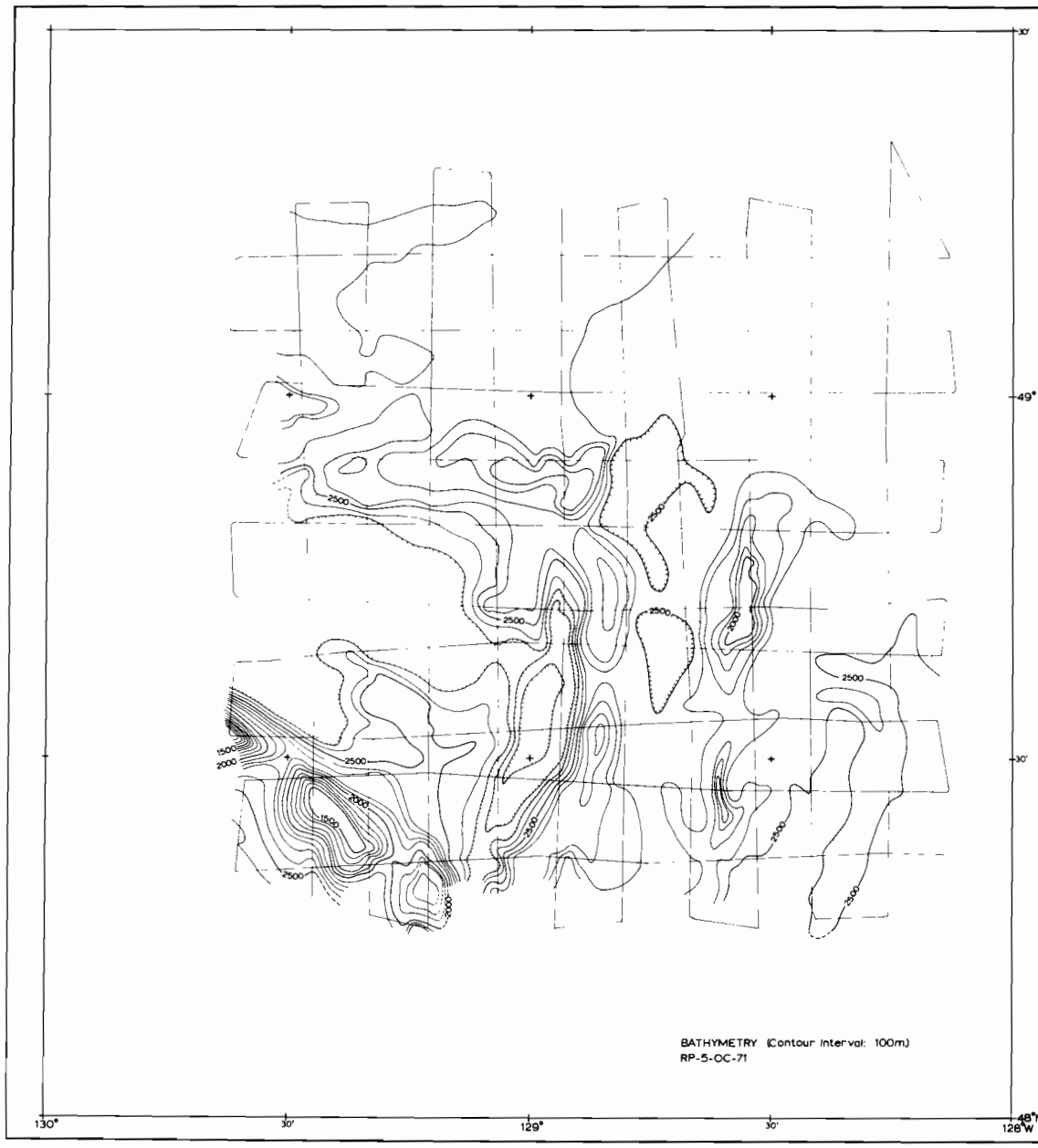

Figure 10. The bathymetry of the ocean floor on, and adjacent to, the north end of the Juan de Fuca Ridge. Depth is expressed in meters. Also shown are the ship's track from which the bathymetric data were collected.

The NW-SE trending structures in the southwest corner of the area are part of a chain of seamounts (Heck Seamounts) which trend northwestward across the Juan de Fuca Ridge south of the local area of this investigation. The shoalest seamount in the surveyed area rises to within 1200 m of the surface. The chain of seamounts appear to have a peripheral depression or moat which is expressed by the 2500 m contour.

The northern part of the area is extremely flat. The basement structure is buried beneath the turbidite sediments of the Cascadia abyssal plain that overlie a thick sequence of pelagic sediments. The topography has been described by Hurley(1960) and McManus (1964).

5.3 Gravity

The free-air anomaly map (fig. 11) has a contour interval of 10 mgals. The contours strongly parallel the bathymetric features (fig. 10) of the Juan de Fuca Ridge, Heck Seamounts and Sovanco Fracture Zone.

The Juan de Fuca Ridge is marked by a pronounced linear gravity feature which exhibits a -40 mgal anomaly flanked by positive anomalies. The negative anomalies follow the flat bottom topographic depression between the two ridge crests.

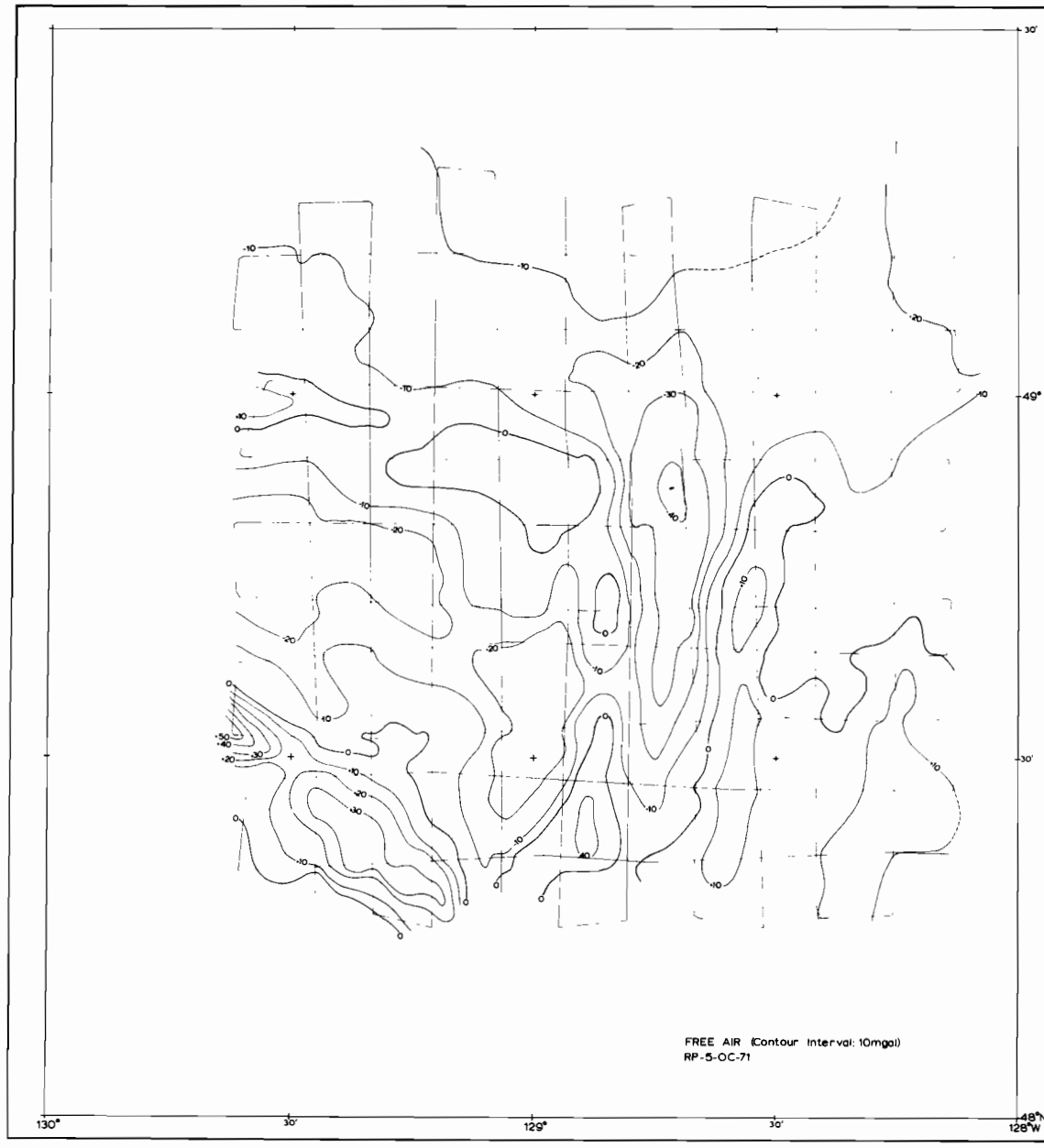

Figure 11. Free-air gravity anomaly map. The values shown in the contour enclosures are the largest or lower values in tens of milligal. Also shown are the ship's track from which gravity data were collected.

Free-air anomalies range from +54 mgals on the Heck Seamounts to -40 mgals over the median depression of the Juan de Fuca Ridge. Slightly negative anomalies (-10 mgals) occur over most of the areas where the topography is relatively flat.

5.4 Magnetics

Residual IGRF magnetic anomalies were contoured at an interval of 100 gammas. This interval is sufficient both to delineate the major anomalies and to mask any minor discrepancies caused by diurnal variations. The resultant magnetic anomaly map (fig. 12), shows linear features closely paralleling those of the bathymetry and gravity maps. The largest linear anomalies (up to 900 gammas) occur on the two ridge crests of the Juan de Fuca Ridge and are separated by a -100 gamma anomaly over the median depression. The Heck Seamounts have anomalies which range from +800 gammas near the peaks to -300 gammas on the flanks.

The IGRF may not accurately represent the average field over this region because the net anomaly in the area remains largely positive rather than zero. Raff and Mason (1961) used a second order polynomial fitted to their data as the regional field (Bullard and Mason 1963) whereas the

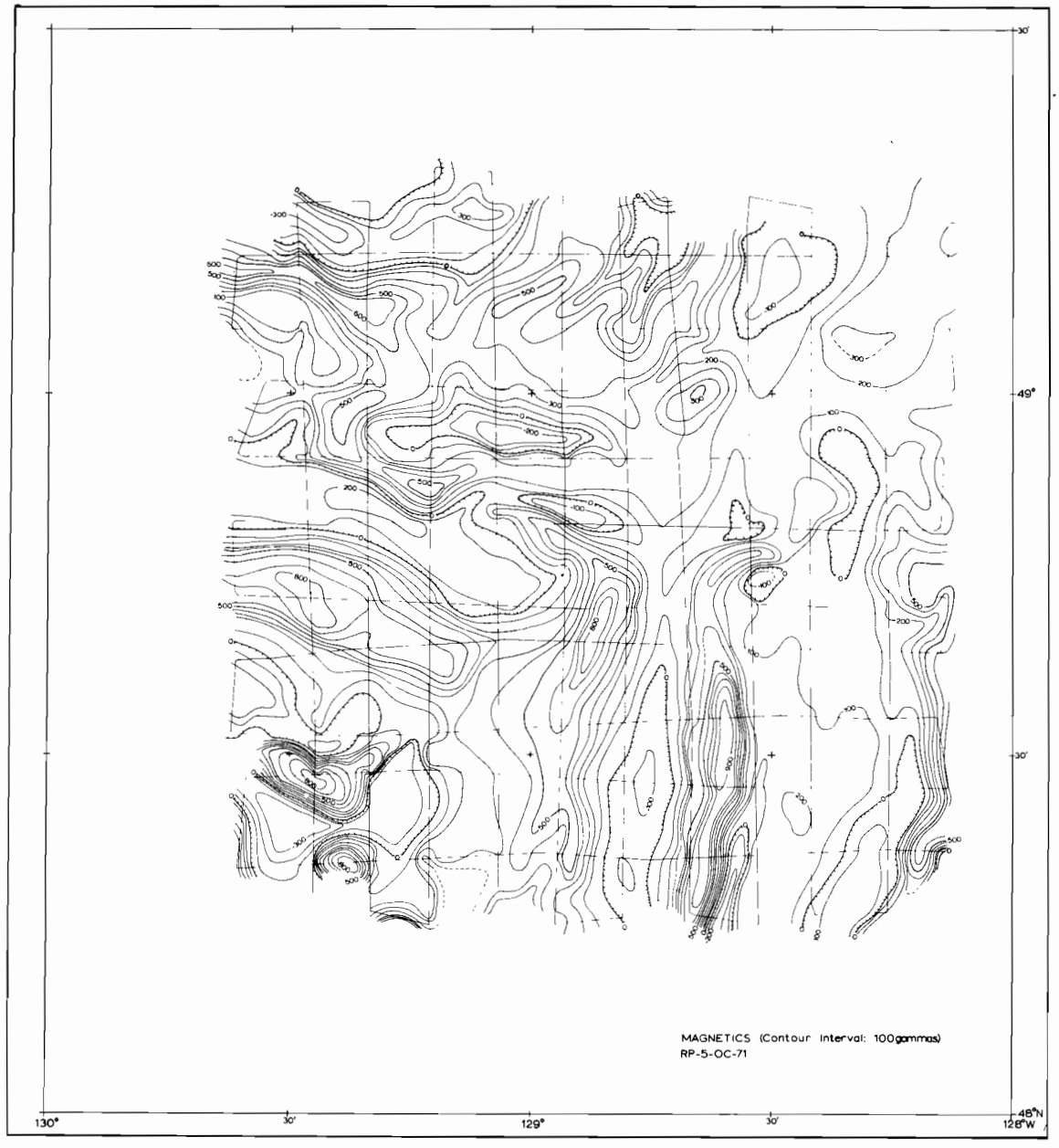

Figure 12. Magnetic anomaly map. Anomalies are calculated using IGRF as regional field. The values shown in the contour enclosure are the largest or lowest observed values in hundreds of gammas. Also shown are the ship's track from which the magnetic data were collected.

regional field (IGRF) used in this report was derived from world wide measurements (IAGA Comm. 2. 1969). Our map indicates a positive bias of approximately 200 gammas.

Raff and Mason (1961) published the results of a marine magnetic survey over the Juan de Fuca ridge, which according to Menard (1964) is part of the mid-ocean ridge system. A detailed tectonic interpretation of these anomalies has been presented by Pavoni (1966) where he shows the Juan de Fuca and Explorer Ridges are displaced about 150 km along a system of faults which he named the 'Sovanco Fault Zone'. If the magnetic chronology is accepted for the Juan de Fuca and Explorer Ridges, separation of the two would have taken place during the past 0.7 m.y. represented by anomaly 1 (Pitman and Heirtzler, 1966; Vine, 1966).

6. ACKNOWLEDGEMENTS

My sincere thanks go to Captain Tonkel and the officers and crew of the OCEANOGRAPHER for their efforts during the project. Although it is difficult to isolate individual contributions, we especially recognize the efforts of CDR Randall and LCDR Vandermeulen in coordinating the overall operation.

I would like to thank R.E. Burns and B.H. Erickson for many valuable discussions and suggestions and R.P. Uhlhorn who assisted in the drafting and Mrs. Kim Hamasaki for typing the manuscript.

7. APPENDIX A

ABSTRACT OF SUCCESSFUL HEAT FLOW OBSERVATIONS

STATION	LOCATION	LATITUDE(N)	LONGITUDE(W)
H004	N7-E10	48°20.0'	128°38.7'
H005	N8-E10	48°21.4'	128°34.0'
H006	N9-E10	48°23.4'	128°26.5'
H007	N10-E10	48°21.7'	128°15.2'
H008	N10-E9	48°28.6'	128°16.0'
H009	N9-E9	48°27.6'	128°26.8'
H010	N9-E9	48°27.5'	128°33.3'
H011	N7-E9	48°27.3'	128°40.3'
H012	N6-E9	48°26.8'	128°48.6'
H013	N5-E9	48°28.0'	128°59.5'
H014	N4-E9	48°28.0'	129°04.6'
H015	N3-E9	48°28.1'	129°13.3'
H016	N1-E8	48°32.8'	129°27.0'
H017	N2-E8	48°31.7'	129°20.6'
H018	N3-E8	48°33.2'	129°13.8'
H020	N5-E8	48°32.8'	128°55.6'
H021	N6-E8	48°33.1'	128°48.0'
H022	N7-E8	48°33.7'	128°41.4'

STATION	LOCATION	LATITUDE(N)	LONGITUDE(W)
HO23	N8-E8	48°33.3'	128°32.2'
HO24	N9-E8	48°34.0'	128°23.4'
HO25	N10-E8	48°33.4'	128°17.0'
HO26	N10-E7	48°38.19'	128°15.6'
HO27	N9-E7	48°40.0'	128°25.7'
HO28	N8-E7	48°39.5'	128°30.1'
HO29	N7-E7	48°39.1'	128°40.6'
HO33	N1-E7	48°38.3'	129°28.0'
HO34	N1-E6	48°43.2'	129°29.5'
HO35	N1-E5	48°48.9'	129°30.3'
HO37	N1-E3	49°01.6'	129°29.6'
HO38	N2-E3	49°01.6'	129°21.3'
HO39	N3-E3	49°01.7'	129°12.6'
HO41	N4-E3	49°00.2'	129°06.9'
HO43	N6-E3	49°00.6'	128°49.9'
HO44	N7-E3	49°01.7'	128°41.4'
3CHO45	N8-E3	49°00.4'	128°32.6'
HO46	N9-E3	49°00.5'	128°24.6'
HO47	N10-E3	49°01.0'	128°16.1'
HO50	N10-E2	49°05.1'	128°15.6'
3CHO51	N1-E10	48°19.9'	129°30.1'
HO54	N2-E9	48°27.9'	129°23.9'

STATION	LOCATION	LATITUDE(N)	LONGITUDE(W)
H055	N5-E10	48°20.5'	128°58.0'
H057	N6-E10	48°21.3'	128°48.3'
H058	N8-E4	48°32.1'	129°05.0'
H059	N4-E7	48°38.7'	129°04.8'
H061	N5-E7	48°37.7'	128°59.9'
H062	N4-E6	48°41.6'	129°04.8'
H063	N4-E5	48°48.1'	129°06.3'
H064	N4-E4	48°54.3'	129°04.0'
H065	N5-E5	48°49.7'	128°56.3'
H066	N5-E6	48°42.7'	128°54.5'
H068	N6-E6	48°41.8'	128°45.7'
H069	N6-E5	48°49.3'	128°47.6'
H071	N5-E3	48°59.8'	128°55.3'
H072	N5-E2	49°04.2'	128°55.4'
H073	N5-E4	48°53.4'	128°56.3'
H075	N6-E4	48°53.6'	128°48.1'
H076	N7-E4	48°53.8'	128°41.7'
H077	N10-E6	48°43.0'	128°15.1'
H078	N9-E6	48°42.7'	128°23.7'
H079	N8-E6	48°42.3'	128°32.4'
H080	N7-E6	48°42.2'	128°40.1'
H082	N3-E7	48°39.2'	129°13.2'

STATION	LOCATION	LATITUDE(N)	LONGITUDE(W)
H083	N2-E7	48°38.3'	129°18.2'
H084	N3-E6	48°42.3'	129°11.3'
H085	N3-E5	48°48.2'	129°13.1'
H086	N3-E4	48°54.0'	129°11.6'
3CH088	N2-E6	48°42.8'	129°19.6'
H089	N2-E5	48°49.1'	129°19.4'
H091	N1-E4	48°54.5'	129°25.6'
H092	N2-E4	48°54.6'	129°18.6'
H093	N1-E2	49°04.9'	129°27.8'
H096	N2-E2	49°04.8'	129°21.1'
H098	N1-E1	49°10.6'	129°29.4'
H099	N2-E1	49°10.0'	129°19.6'
H100	N3-E1	49°11.2'	129°12.7'
H101	N3-E2	49°05.3'	129°11.8'
H105	N4-E2	49°05.0'	129°03.3'
H106	N4-E1	49°11.2'	129°03.8'
H107	N5-E1	49°11.7'	128°56.8'
H108	N6-E1	49°11.4'	128°48.8'
H109	N6-E2	49°06.0'	128°47.6'
H111	N7-E5	48°49.2'	128°40.1'
H113	N8-E4	48°53.8'	128°32.0'
H114	N9-E4	48°54.9'	128°23.7'

STATION	LOCATION	LATITUDE(N)	LONGITUDE(W)
H115	N10-E4	48°54.4'	128°15.5'
H116	N10-E5	48°48.5'	128°14.3'
H117	N9-E5	48°48.3'	128°24.5'
3CH118	N8-E5	48°48.7'	128°31.5'
H120	N6-E7	48°38.7'	128°46.6'
H121	N7-E2	49°05.0'	128°43.3'
H122	N7-E1	49°11.2'	128°43.4'
H123	N8-E1	49°10.8'	128°32.4'
H124	N9-E1	49°10.8'	128°26.0'
H125	N10-E1	49°10.8'	128°15.3'
H126	N9-E2	49°04.4'	128°33.1'
H127	N8-E2	49°05.5'	128°33.0'
H128)		48°43.0'	128°23.3'
H130)	N8-E6	48°42.1'	128°33.5'
H131)		48°42.3'	128°36.6'
H134)		48°42.8'	128°31.0'

8. APPENDIX B

ABSTRACT OF SUCCESSFUL CORE STATIONS

STATION	LOCATION	LATITUDE(N)	LONGITUDE(W)
3CH030	N4-E8	48°33.6'	129°03.1'
3CH051	N1-E10	48°19.9'	129°30.1'
6C053	N1-E10	48°21.2'	129°28.8'
3CH081	N6-E7	48°38.1'	128°47.7'
3CH088	N2-E6	48°42.8'	129°19.6'
3C104	N4-E2	49°05.1'	129°03.1'
3C110	N7-E5	48°49.2'	128°40.1'
3CH118	N8-E5	48°48.7'	128°31.5'

9. APPENDIX C

ABSTRACT OF SUCCESSFUL CAMERA STATIONS

STATION	LOCATION	LATITUDE(N)	LONGITUDE(W)
P031	N(4-5)-E8	48°33.0'	129°00.9'
P074	N(5-6)-E4	48°53.9'	128°52.4'
P119	N(5-6)-E7	48°39.5'	128°55.3'
P132	N(5-6)-E6	48°41.6'	128°49.6'

10. REFERENCES

Bullard, E. C. and Mason, R. G. 1963. The magnetic field over the oceans. The Sea, Vol. 3, (Editor) M. N. Hill. Interscience Publications, pp. 175-210.

Hurley, R.J., 1960. "The geomorphology of abyssal plains in the northeast Pacific Ocean," Scripps Institution of Oceanography Tech. Rept. (S10 Reference 60-7), 105 pp.

IAGA Commission 2 working Group 4 (analysis of geomagnetic field). 1969. International Geomagnetic Reference Field 1965. J. Geophys. Res. 74, pp. 4407-4408.

Lister, C. R. B. 1970. Measurement of in situ sediment conductivity by means of a Bullard type probe. Geophys. J. Roy. Astron. Soc. 19, pp. 521-532.

McManus, D.A., 1967. Physiography of Cobb and Gorda rises, Northeast Pacific Ocean. Geol. Soc. Am. Bull. 78, pp. 527-546

McManus, D. A., 1964, Major Bathymetric features near the coast of Oregon, Washington, and Vancouver Island: Northwest Science, V. 38, pp. 65-82.

Menard, H.W., 1964. Marine Geology of the Pacific, McGraw-Hill, New York, 271 pp.

Pavoni, N., Tectonic interpretation of the magnetic anomalies southwest of Vancouver Island, Pure Appl. Geophys., 63, 172, 1966.

Pitman, W.C., III, and J. R. Heirtzler, Magnetic anomalies over the Pacific-Antarctic Ridge, Science, 154, 1164, 1966.

Raff, A. D., and R. G. Mason, Magnetic Survey off the west coast of North America, 40°N latitude to 52°N latitude, Bull. Geol. Soc. Am., 72, 1267, 1961

Vine, F. J., Spreading of the ocean floor: New evidence, Science, 154, 1405, 1966.

GPO 842-262